IOSUD - Universitatea Politehnica Timişoara
Şcoala Doctorală de Studii Inginereşti

TITLUL TEZEI

PhD Thesis – Summary

for obtaining the scientific title of doctor at
Universitatea Politehnica Timișoara
in doctoral domain of Electronics, Telecommunications and Information Technologies Engineering

autor ing. Teodor-Octavian PĂCURAR
scientific coordinator Prof.univ.dr.ing. Aldo De SABATA

April 2025

The PhD thesis is structured into six chapters: Chapter 1 emphasizes the importance of electromagnetic spectrum management, a finite resource whose efficient use is essential for modern society. Chapter 2 includes significant aspects of spectral occupancy measurement standards, efficient radio noise measurement methods, and technical solutions for common measurement problems. Chapter 3 presents experimental studies and investigations conducted in an Electromagnetic Compatibility (EMC) laboratory. Chapter 4 analyzes electromagnetic interference identified during investigations, providing technical solutions for optimizing electromagnetic spectrum occupancy and improving noise measurement techniques. Chapter 5 addresses applications of metamaterials and frequency-selective surfaces (metasurfaces), used in electromagnetic wave control, manipulation, and electromagnetic disturbance shielding. Chapter 6 synthesizes the conclusions and contributions of the conducted studies.

1. Introduction

This chapter provides an overview of the general research context, discussing the complex issues related to evaluating and managing the electromagnetic spectrum. It analyses measurement standards and methods along with associated practical challenges.

2. General overview of standards in the field of spectral occupancy measurement

The evolution of wireless communication systems over the past two decades has radically changed the human way of life, with wireless systems being directly involved in humanity's social and economic development. Technological progress, expressed in all areas of the information and communications society, has driven an increased demand for high data transfer rates, thus increasing pressure on the radio frequency spectrum.

To establish rules for managing and utilizing the radio-frequency spectrum, numerous recommendations grouped into international standards have been drafted and published. The field

of radiocommunications aims to ensure a rational, equitable, efficient, and economical use of the radio-frequency spectrum by all radiocommunication services.

The opening chapter presents and discusses aspects of the ITU (International Telecommunication Union) international standard used in radiocommunication research, specifically developed to prevent radio interference among users. It addresses recommendations regarding radio-frequency noise measurement methods, ITU-R SM.1753 [ITU SM1753, 2012], ITU-R SM.2155 [ITU SM2155, 2009], and spectral occupancy measurements, ITU-R SM.2256 [ITU SM2256, 2016].

The ITU-R SM.1753 standard provides uniform and accurate methodologies for measuring radio-frequency noise, emphasizing the identification of noise sources, their characteristics, and measurement methods. The main source of interference is Man Made Noise (MMN), The primary source of interference is man-made noise, differing from natural noise by its less predictable variations. This type of noise dominates the urban and residential radio spectrum. Accurate evaluation of the electromagnetic environment is achievable by classifying noise types, using appropriate measurement equipment and procedures. Proper selection of measurement locations, adaptation to noise types, and inclusion of correction factors for measurement uncertainty significantly contribute to preventing interference and optimizing electromagnetic spectrum use, crucial for the evolution of modern communications.

The ITU-R SM.2155 standard identifies several common potential issues arising during spectral occupancy measurements in the high-frequency range (3 - 30 MHz) and provides technical solutions to avoid or mitigate their effects. The measurement process includes a preliminary scan to identify free frequencies, using the same resolution bandwidth (RBW) as the main measurement and applying a RMS (Root Mean Square) detector [ITU SM2155, 2009]. The frequency measured with the lowest signal intensity level is considered the frequency of interest for subsequent measurements. For accurate evaluation of electromagnetic spectrum noise in high-frequency ranges, the standard recommends repeating measurements every 5 minutes.

The ITU-R SM.2256 standard proposes methods for the evaluation of spectral occupancy, defining essential measurement parameters such as measurement threshold, which determines whether a communication channel is free or occupied. A frequency channel is considered occupied if the measured signal level exceeds the threshold level.

Another important parameter in evaluating spectral occupancy is Spectrum Resource Occupancy (SRO), which indicates the ratio between the number of used channels and the total number of available channels within a frequency band. If measuring a single frequency channel, the spectrum resource occupancy equals the channel occupancy frequency. The frequency channel occupancy (FCO) is determined individually for each channel. A frequency channel is considered occupied when any of the samples within that channel exceed the determined threshold.

A crucial aspect when measuring multiple channels or entire frequency bands is separating emissions from adjacent channels, despite their varying levels. If an excessively large measurement bandwidth is used, a strong emission can cause adjacent channels to appear occupied [ITU SM2256, 2016].

3. Measurements and Applications in Electromagnetic Compatibility

The electromagnetic compatibility of electronic systems within modern vehicles has gained significant importance due to the global trend in the automotive industry to replace fossil fuel-powered vehicles with electric ones. Technological advancements directly influencing vehicle functionality have introduced new potential issues related to radiated emissions, leading to increased Man-Made Noise (MMN) spectrum occupancy, as well as challenges in testing internal automotive systems to limit radiated emissions.

In this chapter, results are presented from studies conducted in an electromagnetic compatibility (EMC) laboratory, focusing on emissions generated by vehicles. The primary goal was to identify frequency bands and the intensity of emitted electromagnetic signals through EMC testing to assess their impact on ambient electromagnetic noise levels.

Validating electromagnetic compatibility in vehicles involves successfully passing immunity and electromagnetic emission tests. Given the advancement of electronic systems within vehicles, immunity testing aims to ensure high safety standards for drivers, passengers, and other road users operating within a shared electromagnetic environment [Silaghi, 2016, 1].

In subsection 3.2, I reported a case study on electromagnetic radiation immunity testing in the automobile industry. The investigation demonstrates the necessity of precisely knowing the parameters of measurement equipment, which are prone to change over time due to aging and intensive usage. This understanding ensures the accuracy of electromagnetic field measurements during radiated immunity tests.

The variation of the VSWR parameter of helical antennas used in measurements within the frequency range of 26 MHz to 360 MHz prompted the implementation of solutions to enhance the reliability of radiated immunity tests in an EMC laboratory.

Initially, a type I connector was inserted between the measurement cable in the test configuration and the antenna's ground plane, but this did not yield satisfactory results in relation to the maximum measurement limits of 3:1 required for helical antennas, necessitating the implementation of another solution. Using a directional coupler from Werlatone as a connector on its direct path improved VSWR parameter values. I proposed a third solution employing the calibration kit manufactured by Rohde & Schwarz as a connector between the antenna's ground plane and the measurement cable. The impact of each connector solution on the VSWR results from all three proposed approaches is illustrated in Figure 1. It can be observed that using the directional coupler as a connector resulted in the lowest VSWR values.

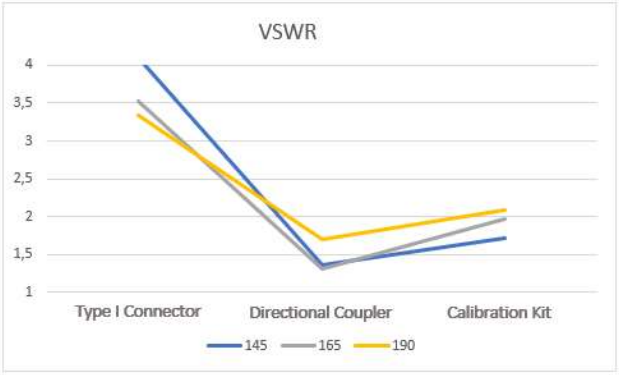

Figure 1. Variation of VSWR using different types of connectors

Figure 2 presents the Smith chart for the NMHA 145 MHz antenna. The antenna impedance shown in this graph was subsequently used in the design of matching networks.

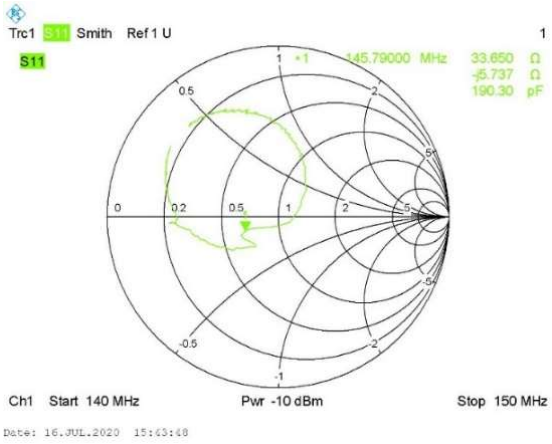

Figure 2. Smith Chart for the 145 MHz NMHA Antenna

Electromagnetic compatibility tests performed in the automotive industry involve determining the emissions generated by each individual device developed, known as a DUT (Device Under Test). To conduct these experiments, additional equipment is required, such as communication modules, other in-vehicle systems, or connecting cables that must closely simulate the vehicle's behavior under normal operating conditions. Under these circumstances, the measurements reflect the emissions of the entire system, not just those of the DUT. The emissions typically correspond to resonant frequencies. Therefore, identifying the resonant frequencies of the entire system is crucial.

In subsection 3.3.1, I described an experimental procedure to measure the resonance frequencies in cables, with the purpose of evaluating the emissions generated by each device under test. The experimental setup used to measure cable resonance is illustrated in Figure 3, while the result of the spectrum analyzer measurement, following the implementation of the proposed solution, is presented in Figure 4.

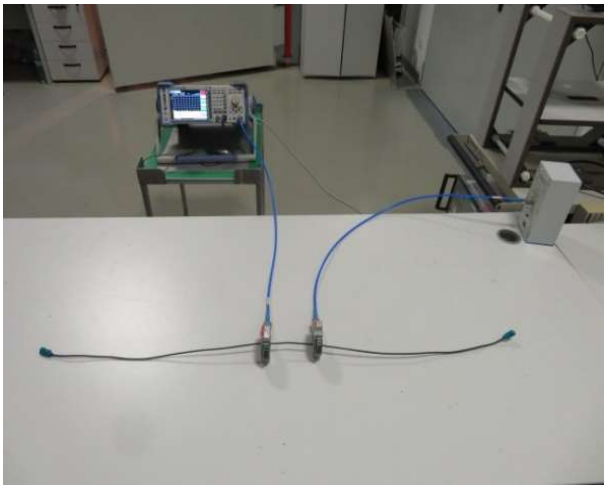

Figure 3. Experimental setup for measuring the resonant frequency in cables

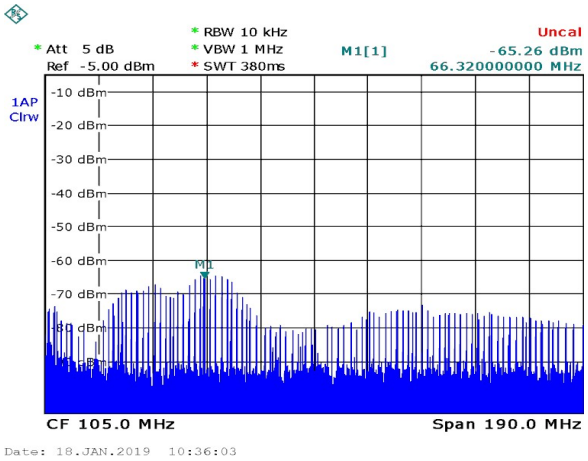

Figure 4. Measurement result with spectrum analyzer:
X- axis: Frequency (MHz); Y-axis- Field intensity (dBm)

Radiated emissions in the 100 kHz – 30 MHz frequency range were measured using a monopole antenna, with the results displayed in Figure 5. The technique used focused on identifying the resonance frequencies in cables using current probes attached to the measurement cable to capture the induced signals. This approach facilitated the correction of anomalies observed during the measurement process, and the results confirmed compliance with limits across all three detectors: black for peak values, blue for quasi-peak values, and red for average value

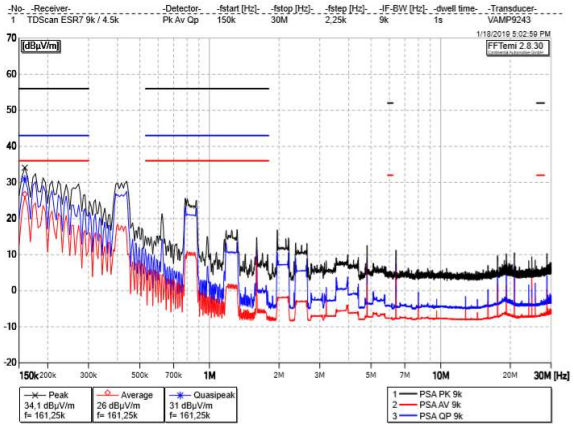

Figure 5. Radiated emissions measurement with Monopole Antenna:
X- axis: Frequency (MHz); Y-axis- Electric Field intensity (dBµV/m)

In subsection 3.3.2, I proposed and investigated several methods to improve the repeatability of radiated emissions (RE) testing for frequencies below 30 MHz. These proposals were made in the context of Annex J of the CISPR 25 standard [CISPR25, 2016] and are intended to improve testing practices in the automotive industry.

Annex J of the CISPR standard, entitled "Validation of ALSE (Absorber Lined Shielded Enclosure) chamber performance 150 kHz - 1 GHz," specifies the requirements for validating semi anechoic chambers used for component tests [cispr25, 2016]. This validation is necessary because, in many cases, test results obtained in different semi-anechoic chambers vary due to differences in chamber dimensions, ground plane sizes and grounding, and the type of absorbing material used.

An initial measurement, prior to applying any methods to improve the results, revealed many points beyond the tolerance limits, as shown in Figure 6. These results represent the equivalent electric field intensity, considering the antenna factor (monopole antenna) and the field emitted by the radiator. The values must fall within the +6 dB and -6 dB limits, as required by Annex J of CISPR 25 [CISPR 25, 2016].

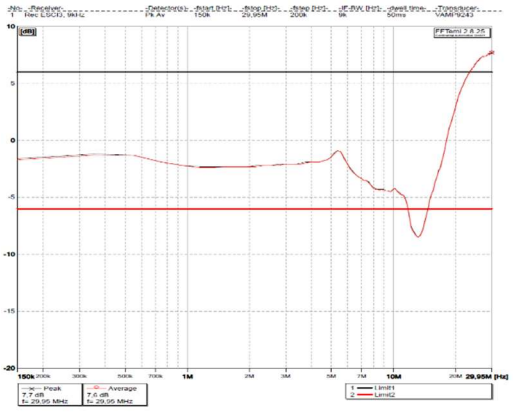

Figure 6. Initial measurement [Silaghi, 2019]: X-axis: Frequency (MHz);
Y-axis: Equivalent Electric Field Intensity (dBµV/m)

The issue was identified as originating from the resonance of the monopole antenna's ground plane [Uno, 2018]. According to [Uno, 2018] and [Carobbi, 2018], the following measures were taken: placing RF absorber pyramids under the monopole antenna, implementing a larger ground plane for the monopole antenna, and strengthening the grounding connection from the counterweight to the ground.

The results reported in Figure 7 are the best obtained and indicate that the problem was solved by applying metal strips to the counterweight, which improved the repeatability of the measurements.

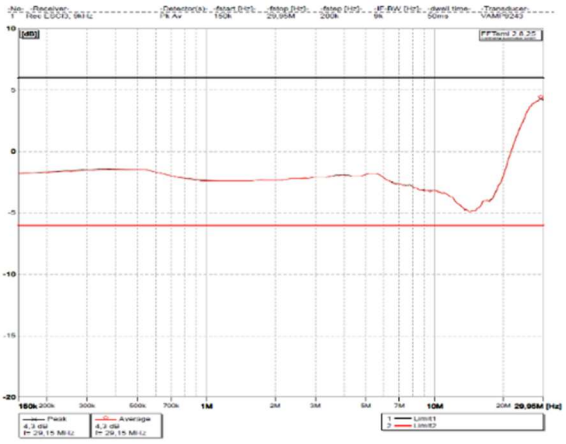

Figure 7. The measurement result with metal strips added to the antenna counterweight [silaghi, 2019]:
X-axis: Frequency (Hz); Y-axis: Equivalent Electric Field Intensity (dBµV/m)

Finally, I applied this solution during a standard radiated emissions measurement test, which led to a reduction in peak electric field intensity levels and eliminated testing errors caused by the test enclosure. This solution is now integrated into the regular operations of the Electromagnetic Compatibility laboratory.

In subsection 3.4, the level of radiated electromagnetic emissions produced by a head-up display device for road vehicles was evaluated based on far-field and near-field electromagnetic field measurements.

Several investigation sessions were conducted in this study. In the initial stage, a far-field radiated emissions measurement was performed, as shown in Figure 8. Subsequently, to identify the origin of the radiation sources, a near-field scan was carried out, Figure 9, followed by the application of a shielding technique aimed at reducing radiated emissions based on the near-field measurements, Figure 10.

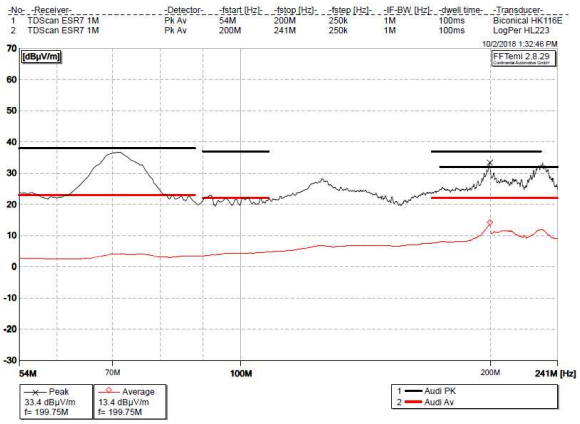

Figure 8. Initial far field measurement [pacurar, 2019]: X-axis: Frequency (Hz);
Y-axis: Electric Field Intensity (dBµV/m)

Near-field scanning, using the EMSCAN measurement system, allowed for the identification of disturbance emission areas on the investigated printed circuit board (PCB). The initial step in locating these emission sources involved superimposing the device's top and bottom layers.

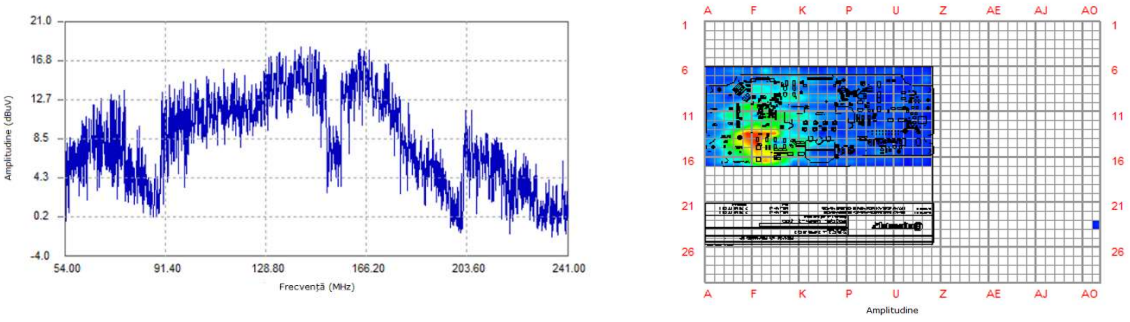

Figure 9. Spectral and Spatial scanning in near field [pacurar,2019].

The final result of the far-field measurement is illustrated in Figure 10, where the signal levels acquired using peak and average detectors are shown to be below the specified measurement limits, resulting in the test being marked as compliant.

Applying a shield to the DC-DC converter of the display power supply proved to be an effective solution, as evidenced by both far-field and near-field scans. Shielding as a method to reduce electromagnetic radiation is widely used due to its high efficiency and low implementation cost. The concept of near-field scanning of the DUT helps significantly reduce the time required to identify design flaws.

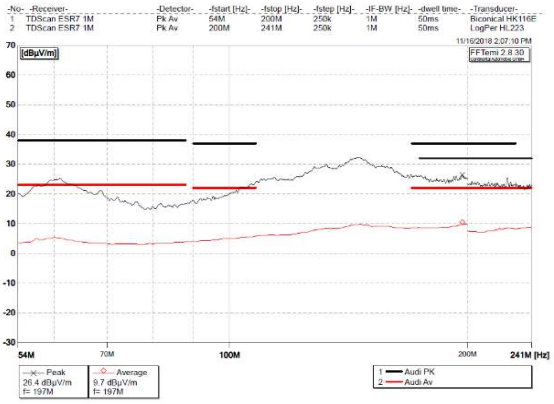

Figure 10. Final far field measurement [pacurar,2019]:
X-axis: Frequency (Hz); Y-axis: Electric Field Intensity (dBµV/m)

In subsection 3.5 I reported a study on the measurement configuration of NFC communications, which operates at a working frequency of 13.56 MHz, with the aim of determining the influence of this communications band on the electromagnetic spectrum. The NFC communications technology installed in many vehicles may interfere with other radio modules inside them, causing vehicle malfunctions.

The measurements performed highlighted the significant influence of the test setup, antenna type, and antenna placement on the investigation results. Figure 11 illustrates the measurement configuration, including the spatial arrangement of the device under test and the antennas. The setup involves two different antenna types—a monopole and a loop—both suited for capturing electromagnetic fields in the 9 kHz to 30 MHz frequency range.

For far-field measurements conducted at 13.56 MHz, the expected ratio between the electric field component (Ex) and the magnetic field component (Hz) is 377 Ω, corresponding to 51.8 dBΩ in logarithmic terms. The results emphasize the impact of electromagnetic interference, particularly the reflections caused by the metallic floor of the semi-anechoic chamber, on the accuracy of measurements taken with both antennas

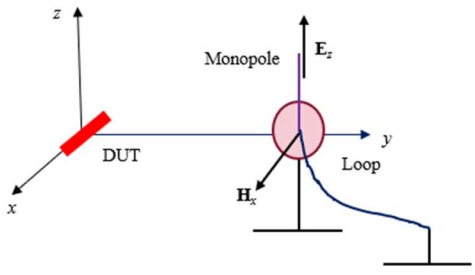

Figure 11. Spatial placement of the DUT and antennas. [pacurar,2022]

4. Spectral occupancy measurements

Chapter 4 addresses and provides solutions to the problems encountered by users of radio communications, most of which originated from human activity. This activity has led to an increase in sources of electromagnetic interference both indoors and outdoors, altering the nature of man-made noise [Fockens, 2019].

Current research on electromagnetic interference and man-made noise is mainly focused on radio noise within industrial environments, where its significance is determined by the increasing number of electrical and electronic devices present [Leferink, 2010], [Angskog, 2010].

In subsection 4.2 I presented a series of measurements conducted within an Electromagnetic Compatibility (EMC) laboratory covering the frequency range of 200 to 3000 MHz. The evaluation of noise power density confirmed significant differences between the various rooms where the measurements were performed. Figure 12 illustrates the experimental setup used for noise measurements, considering the influence of the antenna, cable, and preamplifier on the results

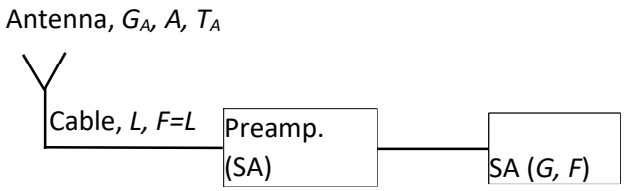

Figure 12. Noise measurement setup [pacurar,2020,2]

Figure 13 presents the results of applying an alternative method for determining noise within the signal-of-interest spectrum, based on sorting signal samples.

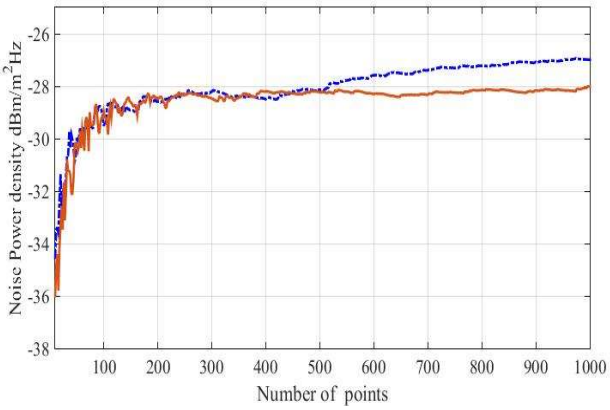

Figure 13. Noise level function of number of measure points [pacurar,2020,2]

In Subsection 4.3, I introduced and described a measurement system built on a Software-Defined Radio (SDR) platform, equipped with a PCB log-periodic antenna. This system was designed to measure electric field intensity and evaluate the occupancy of the electromagnetic spectrum within the 2.4–2.5 GHz range, which is relevant for Wi-Fi communications. The

antenna's behavior was simulated using specialized software, and the resulting parameters were used to calibrate the receiver, thereby enhancing the accuracy of electric field measurements.

I calculated the frequency spectrum occupancy based on the energy threshold detection criterion, following the 3-Sigma rule. This rule states that an interval of ±3σ around the mean of the noise distribution includes 99.7% of the values in the case of a Gaussian distribution, and at least 90% for other types of distributions—a concept illustrated in Figure 14.

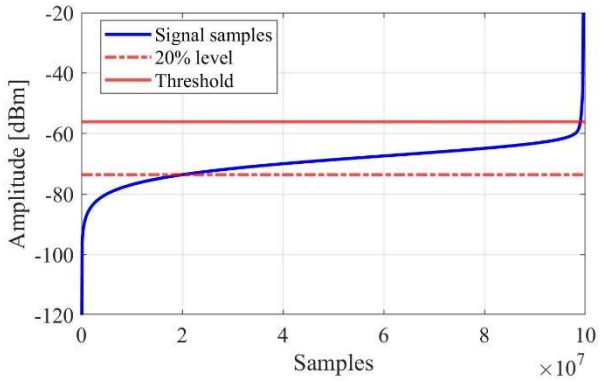

Figure 14. Sorted samples and threshold level [pacurar,2020,1]

The operation of the receiving equipment was demonstrated through time-frequency representations (Figure 15) and spectra of signals acquired from various directions and orthogonal polarizations (Figure 16).

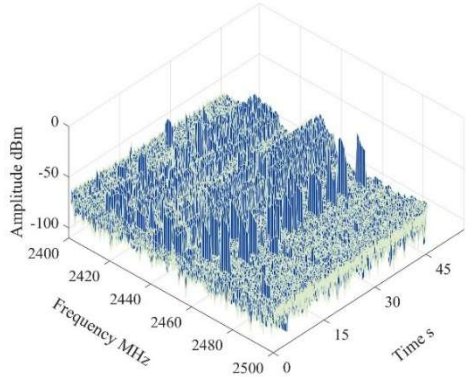

Figure 15. Time-frequency plot [pacurar,2020,1]

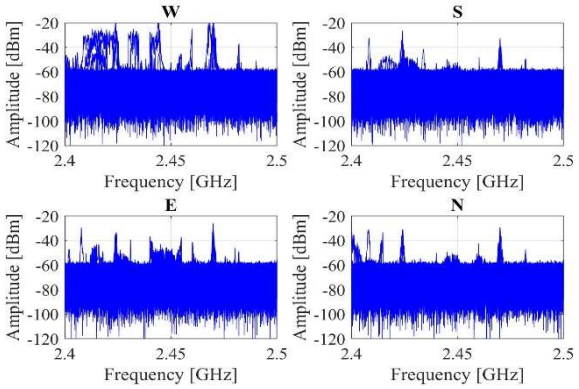

Figure 16. The spectrum of the signal from the four geographical directions [pacurar,2020,1]

Applying cognitive radio concepts to communication systems in the high-frequency (HF) band requires empirical knowledge of the noise levels within the 3–30 MHz frequency range [Fockens, 2019], along with the development of spectrum occupancy (SO) or spectrum availability models. Numerous procedures for measuring spectral occupancy have been proposed, evaluated, and widely discussed in the literature [Wellens, 2010], supported by extensive measurement campaigns in various global locations [Mostafa, 2017], [Haralambous, 2017], [Percival, 1997].

The results presented in subsection 4.4 confirm the ability of modeling the occupancy state of a radio channel at a remote location based on local measurements, utilizing Markov models.

As part of this investigation, I defined two distinct conditional probabilities—one in the time domain and the other in the frequency domain. The proposed models were validated by comparing them with real measurement data collected using GPS-synchronized equipment in two different locations, Timișoara and Sibiu, employing identical measurement systems (Figure 17).

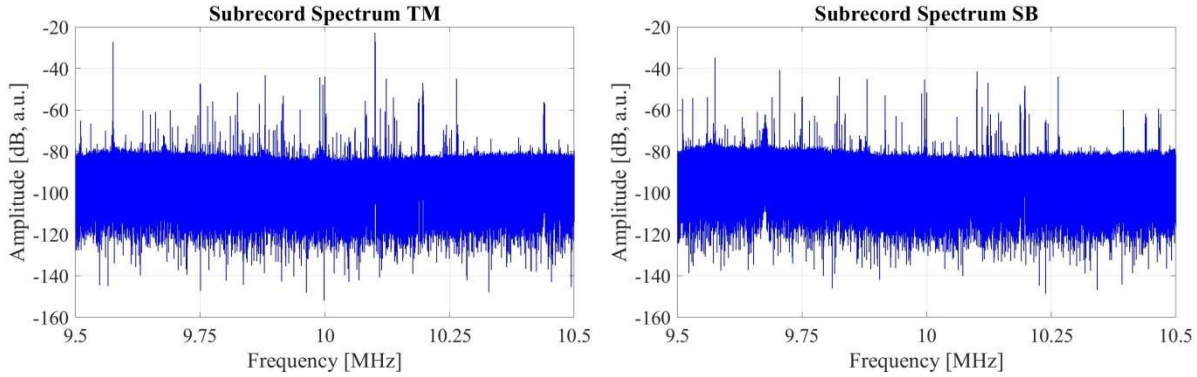

Figure 17: Simultaneous spectrum for the two locations

Figure 18 illustrates the conditional probability in the frequency domain for two separate bands. For comparison, the conditional probability in the time domain is also presented. The close correlation between the two indicates the potential for characterizing a remote radio channel both temporally and across different frequency bands based on locally acquired data.

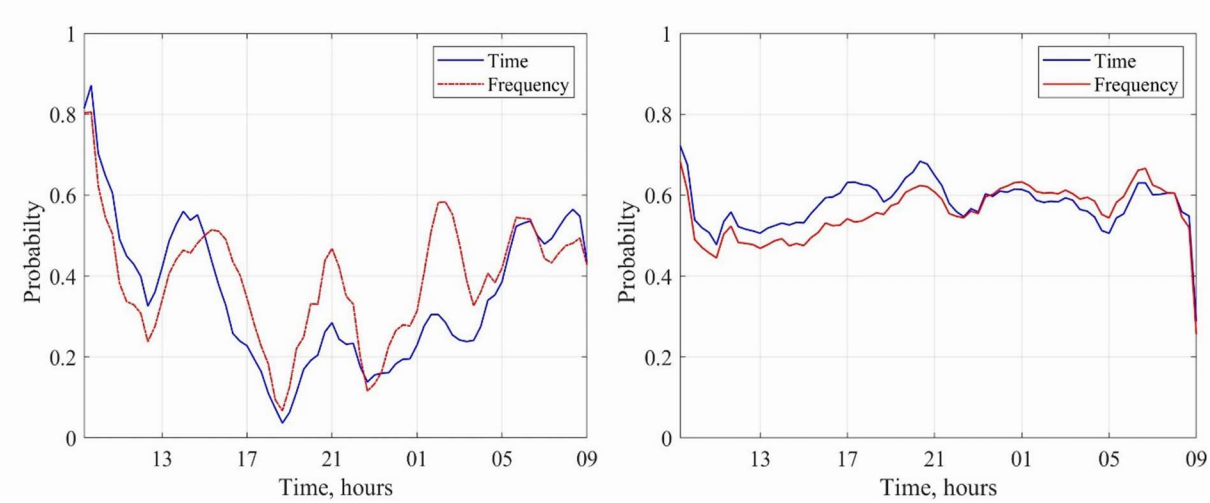

Figure 18: Comparison of conditional probabilities in time and frequency for two frequency bands

5. Electromagnetic shields with frequency selective surfaces

Chapter 5 explores the evolution of metamaterials and volumetric periodic (3D) electromagnetic structures, as well as the paradigm of frequency-selective surfaces (FSS), highlighting some of the most notable achievements in this field of research.

In Subsection 5.1, I developed a liquid-based absorber designed as a fully dielectric frequency-selective surface, except for the ground plane. The first solution utilizes water, chosen for its high real and imaginary permittivity values, which enable both miniaturization and effective absorption. The second, more innovative solution investigates methanol as the absorbing liquid. For both configurations, the geometric dimensions of the unit cell were optimized to enhance performance [Dsa, 2024].

Figure 19 illustrates the design of the liquid-based absorber. The left side (Figure 19 a) shows the CAD model of the water-based absorber unit cell, while the right side (Figure 19 b) presents the methanol-based version. The difference in unit cell size is attributed to the higher dielectric constant of water compared to methanol. The absorber structure is formed by infinitely repeating the optimized unit cell in the xy-plane.

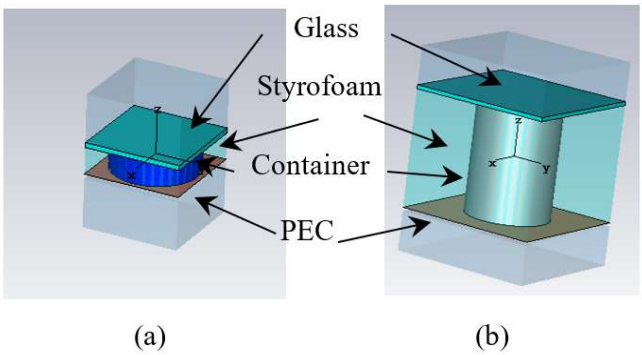

Figure 19. CAD model of the unit cell of the absorber based on liquids:
a) water; b) methanol [Dsa, 2024]

In Figure 20, I presented the real and imaginary components of the permittivity of water and methanol at the temperature of 20 °C, modeled using the Debye approximation. For water, the real part of the relative dielectric constant decreases from 80 to 74 as the frequency increases from 1 GHz to 5 GHz, while the imaginary part rises from 4.5 to 20.5 over the same range. Methanol follows a similar trend: the real part drops from 30.5 to 12.4, and the imaginary part increases from 9 to 12. Notably, methanol exhibits higher dielectric losses than water up to approximately 3 GHz; beyond this frequency, water demonstrates greater losses. This behavior suggests the potential for tuning the absorber's frequency response by selecting the appropriate liquid material [Dsa, 2024].

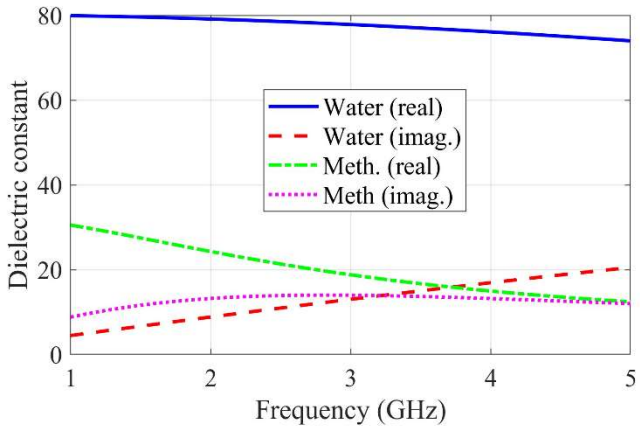

Figure 20. Dielectric constants of water and methanol at 20°C [Dsa, 2024]

To understand the electromagnetic behavior of the water- and methanol-based absorbers, simulations were conducted using a first-order Debye model for both materials, as specified in [CST, 2023]. Additionally, normal-incidence simulations were performed in [HFSS, 2023] at a temperature of 20 °C for both absorber types.

As shown in Figure 21, the simulation results for the water-based unit cell are consistent across both CST and HFSS. For the methanol-based absorber, minor discrepancies appear at higher frequencies, likely due to differences in the implementation of the Debye model—particularly in the coefficients used to extrapolate frequency-dependent permittivity.

According to Figure 21, the water-based unit cell does not show significant differences between the two calculation methods. The methanol-based units indicate minor differences at higher frequencies. These variations can be attributed to differences in the implementation of the Debye model between the two simulators, particularly the coefficients used in the equation for extrapolating relative permittivity data.

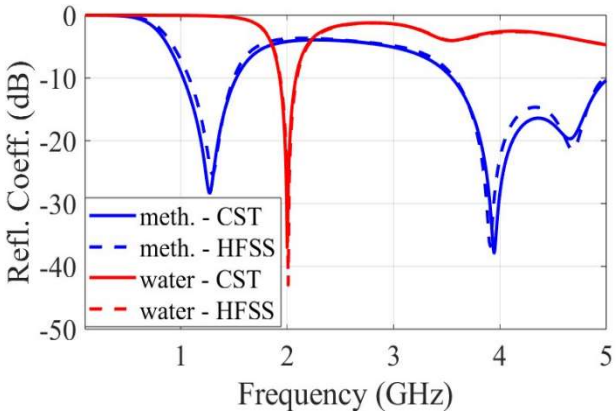

Figure 21. Joint representation of the reflection coefficient obtained by two different simulation software packages [Dsa, 2024]

I demonstrated through simulations that the proposed frequency-selective absorber designs maintain stable reflection coefficients across a wide range of incidence angles, polarizations, and temperatures.

6. Contributtons

During the doctoral program I studied a number of 106 bibliographic titles, leading to 1 ISI- WoS journal publication, 5 ISI Proceedings conference articles, and 1 article at BDI indexed conferences. I enumerate below my own contributions to this thesis:

In chapter 2:

- I presented and discussed key aspects of measurement standards in the field of radiocommunications, with a particular focus on spectral occupancy.
- I introduced and explained a practical method for determining the noise level received by an antenna in the presence of anthropogenic signals—the 20% criterion (Subsection 2.2). This method allows the identification and exclusion of unwanted signals from the frequency spectrum by treating the lowest 20% of sampled values as background noise.
- I synthesized a set of common challenges encountered in high-frequency spectral occupancy measurements and I described the corresponding technical solutions recommended by the ITU-R SM.2155 standard (Subsection 2.3).
- I explored the complexity of managing the electromagnetic spectrum and described the technical guidelines provided by the ITU-R SM.2256 standard for evaluating spectral occupancy (Subsection 2.4).

In chapter 3:

- I conducted practical investigations in an electromagnetic compatibility (EMC) laboratory to assess spectral occupancy measurements for analyzing emissions generated by vehicles. Through EMC tests performed, I demonstrated the impact of vehicles on increasing background electromagnetic noise.
- In Subsection 3.2, I evaluated the influence of measurement equipment and configurations on the validity of radiated immunity testing using helical antennas. Experimental results revealed performance degradation in Type I connectors due to aging and repeated use. To address this, I proposed and validated an alternative solution involving a Werlatone directional coupler, inserted between the antenna ground plane and the signal cable. This approach significantly improved the voltage standing wave ratio (VSWR) and corrected measurement errors attributed to equipment faults.
- I performed a comparison between the nominal and measured parameters of helical antennas, which revealed deviations from manufacturer's specifications, underlining the importance of verifying test equipment performance in EMC setups.
- In Subsection 3.3, I investigated the influence of resonance frequencies on radiated emissions in automotive testing. Using an experimental method involving current probes, I identified cable-induced resonances that impact emission levels—highlighting that emissions can be affected not only by the device under test, but also by cabling and interconnection hardware.

- I applied the 'modeled long wire' method described in Annex J of the CISPR 25 standard, comparing the standard's simulation values with actual measurement data to assess compliance. In the 150 kHz to 30 MHz frequency range, significant deviations from the specified limits were observed. To enhance test repeatability, I implemented a grounding strap on the monopole antenna's counterweight, which effectively reduced peak electric field levels and brought the measurements within compliant thresholds. This solution continues to be used in EMC testing procedures.
- In subsection 3.4, I introduced the EMSCAN technology for near-field scanning of radiated emissions. By applying the near-field scanning method, I accurately identified the sources of interfering emissions through both spectral and spatial scans.
- I proposed and implemented a practical shielding solution for the printed circuit board of the investigated device by applying an aluminum shield to its power circuit. This approach reduced interfering radiated emissions in the 54–241 MHz frequency range by approximately 10 dB. I validated the effectiveness of the shielding by repeating the initial far-field measurements, which confirmed compliance with the limits imposed by the CISPR 25 standard, thereby certifying the device for mass production
- In Subsection 3.5, I compared the performance of two antenna types used in EMC testing within the 9 kHz–30 MHz frequency range, monopole antenna and loop antenna, outlining the advantages and limitations of each based on specific test scenarios.
- I highlighted potential electromagnetic interference (EMI) issues between NFC communication systems operating at 13.56 MHz and other in-vehicle electronic modules functioning within the same frequency band, such as wireless phone charging systems. Furthermore, I demonstrated how EMI reflections from the metallic floor of the semi-anechoic chamber can influence the measurement configuration.

In chapter 4:

- I analyzed the impact of technological advancements on the electromagnetic spectrum and emphasized the exponential increase in man-made electromagnetic noise (MMN). This growing interference affects radio communication users by degrading mobile and Wi-Fi network performance, reducing GPS accuracy in densely populated urban areas, and disrupting communications in frequency bands allocated to safety-critical systems, such as those used by emergency services.
- In Subsection 4.2, I implemented a complex experimental setup incorporating a log-periodic antenna and a high-performance spectrum analyzer to investigate the electromagnetic spectrum within the 200–3000 MHz frequency range. I optimized the measurement method using internal preamplifiers and applying corrections for power losses introduced by the measurement cables.

- I developed a noise spectral density measurement procedure based on a model that integrates noise figure, antenna gain, and noise temperature. This method enables accurate estimation of radio noise levels for dynamic access and spectrum management in cognitive radio networks.
- In Subsection 4.3, I introduced an innovative spectral scanning system based on the HackRF One software-defined radio (SDR), utilizing fast clock retuning techniques to enable efficient frequency scanning. This approach reduced the sweep time to 0.75 seconds across the entire 6 GHz frequency range.
- I proposed an effective energy threshold detection method by applying the 3-Sigma rule in combination with the lowest 20% sample-sorting approach to evaluate man-made noise and spectrum occupancy. I validated the propose method through graphical analysis of spectral data and by comparing measured values with corresponding estimates.
- I conducted an analysis of congestion levels in Wi-Fi communication channels by calculating the duty cycle and occupancy factor for the channels of interest. Detailed graphical representations were provided to highlight areas of high activity.
- In subsection 4.4, I introduced an extended Markov model for statistically analyzing high-frequency spectrum usage across geographically distinct locations, Timișoara and Sibiu, by jointly considering time, frequency, and spatial parameters.
- I implemented a GPS-synchronized experimental setup using SDRs to perform simultaneous spectral measurements at different locations. I created a custom Python script to automate the processing and segmentation of the acquired data, streamlining analysis and improving efficiency
- I used a two-dimensional model for analyzing shared electromagnetic spectrum occupancy by calculating the probability of a frequency channel being occupied based on the state of its adjacent channels. I validated the model through comparative analysis of results obtained from different geographic location

In chapter 5:

- I provided an overview of metamaterials, frequency-selective surfaces (FSS), and metasurfaces, focusing on their fundamental properties and outlining their most impactful applications in electromagnetic engineering.
- In Subsection 5.2, I developed a liquid-based frequency-selective absorber using water and methanol, incorporating a fully dielectric frequency-selective surface (FSS) topology, except for the ground plane. The design was intended for the selective shielding of specific spatial regions.
- I performed detailed simulations of the liquid-based absorber in CST Microwave Studio and validated the results using an alternative electromagnetic simulation tool, HFSS, confirming their accuracy.

- I conducted parametric studies on unit cell dimensions, substrate thickness, and cylinder radius to optimize the absorber's performance. Additionally, I performed a sensitivity analysis to evaluate the effects of incidence angle and polarization on absorption efficiency.
- I analyzed the effects of temperature on the resonance frequency and reflection coefficient, demonstrating the absorber's performance stability across a wide range of temperatures.
- I investigated the resonance mechanisms within the structure by generating electromagnetic field visualizations to analyze the interactions between the fields and the constituent materials, as well as the absorption behavior within the liquid regions of the absorber.

7. References

[Angskog, 2010] P. Angskog, C. Karlsson, J. F. Coll, J. Chilo, and P. F. Stenumgaard, "Sources of disturbances on wireless communication in industrial and factory environments," in *Proc. Asia-Pac. Int. Symp. Electromagn. Compat.*, Beijng, China, Apr. 2010, pp. 281–284,

[Balint,2020] C. Balint, A. De Sabata, **O. Pacurar**, P. Bechet, „Markov Model for HF Joint Spectrum Occupancy at Two Distant Locations", The 26th International Conference

Knowledge-Based Organization (KBO 2020), 11-13 June 2020, Sibiu, Romania, 2020

[Carobbi, 2018] C. Carobbi, D. Izzo, "Evaluation and improvement of the Reproducibility of CISPR 25 ALSE Test Method", IEEE Transactions on Electromagnetic Compatibility, vol. 60, issue 4, pp. 1069-1077, 2018.

[CISPR25, 2016] International Standard CISPR 25, "Vehicles, boats and internal combustion engines - Radio disturbance characteristics ", 4.0 ed. 2016

[CST,2023] CST Microwave Studio, v. 2023

[Dsa, 2024] A. De Sabata, A. Silaghi, C. Ionica, O. Pacurar, "Design of Liquid Based Frequency Selective Surfaces Operating as Absorbers," Advances in Electrical and Computer Engineering, vol.24, no.4, pp.75-82, 2024

[Fockens, 2019] T. Fockens, A. Zwamborn and F. Leferink, "Measurement Methodology and Results of Measurements of the Man-Made Noise Floor on HF in The Netherlands", IEEE Transactions on Electromagnetic Compatibility, Vol. 61, Nr. 2, April 2019, pp. 337-343, 2019

[Haralambous, 2017] H. Haralambous, H. Papadopoulos, 24-h HF spectral occupancy characteristics and neural network modeling over Northern Europe, IEEE Trans. Eletromagn. Compat, vol. 59, no. 6, pp. 1817-1825, Dec., 2017.

[HFSS,2023] High Frequency Structure Simulator (HFSS), www.ansys.com.

[ITU SM1753, 2012] Recommendation ITU-R SM.1753-2 Methods for measurements of radio noise, ITU-R 2012.

[ITU SM2155, 2009] ITU R-SM 2155 09/2009 Man made noise in the HF range

[ITU SM2256, 2016] ITU-R SM.2256-1 Spectrum occupancy measurements and evaluation

[Leferink, 2010] F. Leferink, F. Silva, J. Catrysse, S. Batteman, V. Beauvois, and A. Roc'h, "Man-made noise in our living environments," URSI Radio Sci. Bull., vol. 83, no. 3. pp. 49–57, Sep. 2010.

[Mostafa, 2017] Md.M. Mostafa, E. Tsolaki, H. Haralambous, HF spectral occupancy Time Series models over the Eastern Mediterranean Region, IEEE Trans. Eletromagn. Compat, vol. 59, no. 1, pp. 240-248, Feb., 2017.

[Neiconi, 2020] A. Neiconi, **O. PACURAR**, A. De Sabata, „EMC Parameters used for Helical Antennas in Automotive EMC Testing", 5-6 November 2020, Timisoara, Romania

[Pacurar, 2022] **O. Pacurar**, A. Silaghi, C.Balan, A.De Sabata, C.Balint, "Study regarding the configuration setup used inside an EMC Laboratory for NFC Communication Measurement", 2022 IEEE 28th International Symposium for Design and Technology in Electronic Packaging (SIITME), 26-29 October 2022, Bucharest, Romania

[Pacurar, 2020,1] **O. Pacurar**, C. Balint, C. Iftode, A. Silaghi, A. De Sabata, "Spectrum Occupancy Measurements in the Wi-Fi Band with a PCB Antenna", 2020 14th International Symposium on Electronics and Telecommunications (ISETC 2020), 5-6 November 2020, Timisoara, Romania, pp. 1-4, 2020

[Pacurar, 2020,2] **O. Pacurar**, A. Silaghi, C. Balint, A. De Sabata, Adrian Graur, "Experiments Concerning the Spectrum Structure Inside an Automotive EMC Laboratory", 2020 International Conference on Development and Application Systems (DAS 2020), 21-23 May 2020, Suceava, Romania, pp. 133-136, 2020

[Pacurar, 2019] **O. Pacurar**, A. Silaghi, A. De Sabata, „Aspects regarding radiated emissions produced by a head up display", 2019 IEEE 25th International Symposium for Design and Technology in Electronic Packaging (SIITME 2019), 23-26 October 2019, Cluj, Romania, pp. 30-33, 2019

[Mostafa, 2017] **Md.M. Mostafa**, E. Tsolaki, H. Haralambous, HF spectral occupancy Time Series models over the Eastern Mediterranean Region, IEEE Trans. Eletromagn. Compat, vol. 59, no. 1, pp. 240-248, Feb., 2017.

[Silaghi,2016,1] A. Silaghi, A. De Sabata, A. M. Silaghi, "Testing Immunity to Portable Transmitters with Helical Antennas: Key concepts", SIITME 2016, 20-23 Oct2016, Baile Felix (Romania), pp. 270-273, 2016

[Uno, 2018] T. Uno, K. Maeda, T. Tanaka, Y. Okuda, O. Wada, “A study on characteristics of 10 MHz to 30 MHz in CISPR 25 ALSE method: CISPR 25 Annex J reference data verification of long-wire method”, 2018 IEEE International Symposium on Electromagnetic Compatibility and 2018 IEEE Asia-Pacific Symposium on Electromagnetic Compatibility (EMC/APEMC), 14-18 May 2018, Singapore (Singapore), pp.584-589, 2018.